Progress In Electromagnetics Research, Vol. 124, 441–455, 2012

SYNTHESIS OF MICROWAVE RESONATOR DIPLEXERS USING LINEAR FREQUENCY TRANSFORMATION AND OPTIMIZATION

R. Wang*, J. Xu, M.-Y. Wang, and Y.-L. Dong

School of Physical Electronics, University of Electronic Science and Technology of China, No. 4, Section 2, Jian She North Road, Chengdu 610054, China

Abstract—This paper presents a method for synthesizing coupled resonator diplexers composed of TX and RX filters (two types of junctions connecting the TX and RX filters are considered). For the first junction type, the common port is directly coupled to the first resonator of the TX and RX filters, respectively. For the second junction type, common node is realized by adding an extra resonator besides those of the TX and RX filters. The method is based on the evaluation of the characteristic polynomials of the diplexer using the proposed linear frequency transformation and well-established method, and then the "$N + 3$" coupling matrix of overall diplexer can be obtained using hybrid optimization methods. Two diplexers have been designed and fabricated to validate the proposed method.

1. INTRODUCTION

Microwave diplexers are important components in mobile communication systems. They are typically applied to transmit and receive signals by a single antenna. A diplexer can also be used to separate a composite signal coming from a common port into two channel signals to permit each signal to be transmitted separately. Because of the interaction of the two filters composing the diplexer, the characteristics of a diplexer are different from the responses of the individual two filters. The complexity of the interaction makes the design of a diplexer complicated.

For the design of microwave diplexers, the traditional approach to is to design the TX and RX filters individually and then to design a

Received 11 January 2012, Accepted 2 February 2012, Scheduled 8 February 2012

* Corresponding author: Rui Wang (rfywr@yahoo.com.cn).

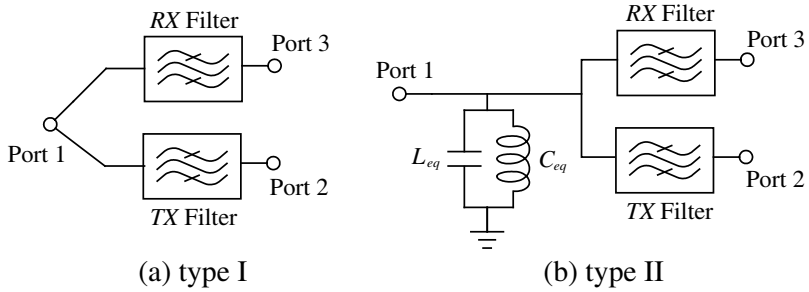

Figure 1. Different diplexer junctions considered in this study. (a) Type-I junction. (b) Type-II junction.

distribution network. The most employed distribution network used today may be the T-junction (as in [1–5]) connecting the TX and RX filters. The diplexer with the T-junction configuration has drawbacks of large volume and time-consuming. Some interesting diplexers design without distribution networks have appeared in the recent literatures [6–12]. A new topology of the diplexer with the common port directly connected to two filters was proposed and synthesized in [7], although no design example was given. Figure 1(a) shows this new structure proposed in [7]. In [6], the diplexers employing an extra resonant junction [an extra resonator in addition to the channel filters, shown in Figure 1(b)] has been synthesized based on the evaluation of the characteristic polynomials of the diplexer and similarity-transformation. A design procedure for coupled resonator diplexers that do not employ any external junctions was also reported in [8], and was further verified in [9]. The method in [8] is based on gradient optimization technique. However, the gradient of the objective error function was not given and asymmetric responses of the diplexers were not synthesized. In addition, the diplexer structures proposed in [8, 9] has poorer isolation than that shown in Figure 1. In [10–12], miniaturized microstrip resonators diplexers designed using common resonator sections have been proposed. These common resonator sections must have two resonant frequencies, playing roles as the one resonator of the TX and RX filters, respectively. In fact, these compact diplexer structures can be described using Type-I junction shown in Figure 1(a).

In this paper, a method is presented for coupling matrix synthesis of overall resonator diplexer with two types of junctions, which represent a large class of practical diplexers implementations. The equivalent circuits of these junctions are shown in Figure 1. These two categories of diplexers do not require T-junction. Type-I diplexer has

compact circuit size. When two resonators coupled to common port 1 are replaced one resonator with two resonant frequencies (such as SIR in [10] and T-shaped resonator in [11]), the size of Type-I diplexer can be further reduced. Type-II diplexer has characteristics of easy implement and high isolation, although its configuration has drawbacks of large volume due to adding an extra resonator. For a designer, either of two types of diplexers can be chosen according to filter technology, electrical requirements, mechanical constraints, and so on.

The proposed method is based on the evaluation of the characteristic polynomials of the diplexer using the proposed linear frequency transformation and established method in [6], and then coupling matrix of overall resonator diplexer can be obtained using the proposed hybrid optimization methods. Using the technique described in this paper, there is no need to master all the different existing similarity-transformation-based techniques. Two diplexers has been designed, fabricated and measured to verify the proposed method.

2. CALCULATION OF DIPLEXER CHARACTERISTIC POLYNOMIALS

The S-parameters of the two low-pass prototype filters (RX and TX) in the normalized frequency Ω domain ($s = j\Omega$) can be expressed through their characteristic polynomials as [6, 13]:

$$\begin{aligned} S_{11}^{TX} &= \frac{F_{TX}(s)}{E_{TX}(s)}, \quad S_{21}^{TX} = \frac{P_{TX}(s)}{E_{TX}(s)} = \frac{p_{0TX} P_{TXn}(s)}{E_{TX}(s)} \\ S_{11}^{RX} &= \frac{F_{RX}(s)}{E_{RX}(s)}, \quad S_{21}^{RX} = \frac{P_{RX}(s)}{E_{RX}(s)} = \frac{p_{0RX} P_{RXn}(s)}{E_{RX}(s)} \end{aligned} \tag{1}$$

The polynomials $E_{TX}(s)$ and $F_{TX}(s)$ have degree N_{TX} (order of TX filter), the polynomials $E_{RX}(s)$ and $F_{RX}(s)$ have degree N_{RX} (order of TX filter). The TX and RX transmission zeros can completely define the polynomials $P_{TXn}(s)$ and $P_{RXn}(s)$. The coefficients p_{0TX} and p_{0RX} are determined by the return loss at the passband [13].

The S-parameters of the diplexers can be defined using four polynomials in s domain as [6]

$$S_{11} = \frac{N(s)}{D(s)}, \quad S_{21} = \frac{p_{0t} P_t(s)}{D(s)}, \quad S_{31} = \frac{p_{0r} P_r(s)}{D(s)} \tag{2}$$

The highest degree coefficient of $N(s)$, $D(s)$, $P_t(s)$, and $P_r(s)$ is imposed equal to 1 with p_{0t} and p_{0r} suitable normalizing coefficients. Note that the definition of S_{11} is different from that in [6]. It is no necessary for two-type junction diplexers in Figure 1 to multiply the polynomial $N(s)$ by a coefficient.

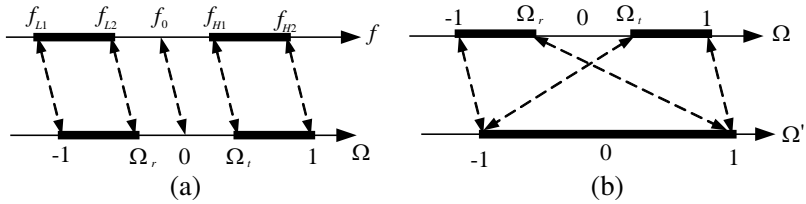

Figure 2. (a) Frequency mapping from Ω domain to f domain from [6], and (b) the proposed frequency mapping from Ω' domain to Ω domain.

The synthesis of the diplexer is carried out in a normalized frequency domain Ω, defined by low-pass to bandpass frequency transformation as:

$$\Omega = (f_0/BW)(f/f_0 - f_0/f) \tag{3}$$

where $BW = f_{H2} - f_{L1}$ and $f_0 = \sqrt{f_{L1} \cdot f_{H2}}$. Figure 2(a) shows the correspondence among the relevant frequency points of this transformation [6]. It is assumed that the RX band is below the TX band. The passband limits of the RX filter are represented by f_{L1}, f_{L2}, while those of the TX filter are f_{H1}, f_{H2}. Note that the two inner passbands limits are not, in general, geometrically symmetric with respect to f_0 (consequently $\Omega_r \neq -\Omega_t$).

The initial synthesis of the TX and RX filters provides a very good starting point for the calculation of the characteristic polynomials of the diplexer, so the convergence can be achieved within $5 \sim 10$ iterations [6]. To obtain initial characteristic polynomials of the TX and RX filters in Ω domain, a frequency mapping from Ω' domain to Ω domain is proposed. Figure 2(b) shows the correspondence among the relevant frequency points of the proposed transformation. The TX and RX filters are directly synthesized in Ω' domain using method in [13], and then initial characteristic polynomials of the TX and RX filters in (1) can be obtained by the proposed frequency transformation.

The proposed frequency transformation from Ω' to Ω can be expressed as follows:

$$\begin{array}{ll} \Omega = a_1\Omega' + b_1, & \text{for } RX \text{ filter} \\ \Omega = a_2\Omega' + b_2, & \text{for } TX \text{ filter} \end{array} \tag{4}$$

Since -1 and 1 in the Ω' domain are transformed to -1 and Ω_r in the Ω domain for the RX filter, respectively, and -1 and 1 in the Ω' domain are transformed to Ω_t and 1 in the Ω domain for the TX filter, respectively, we must enforce

$$\begin{cases} -1 = -a_1 + b_1 \\ \Omega_r = a_1 + b_1 \end{cases}, \quad \begin{cases} 1 = a_2 + b_2 \\ \Omega_t = -a_2 + b_2 \end{cases} \tag{5}$$

From (5), the constant in (4) can be expressed as:

$$a_1 = \frac{\Omega_r + 1}{2},\ b_1 = \frac{\Omega_r - 1}{2};\quad a_2 = \frac{1 - \Omega_t}{2},\ b_2 = \frac{\Omega_t + 1}{2} \tag{6}$$

The diplexer polynomials can be derived using the admittances at the input ports of the TX and RX filters, taking into account the interaction between the RX and TX filters through junctions. The following expressions can be obtained:

For Type I junction:

$$\begin{aligned} N(s) &= S_{TX}S_{RX} - D_{TX}S_{RX} - S_{TX}D_{RX} \\ D(s) &= S_{TX}S_{RX} + D_{TX}S_{RX} + S_{TX}D_{RX} \\ P_t(s) &= P_{TXn}S_{RX}, \quad p_{0t} = p_{0TX} \\ P_r(s) &= P_{RXn}S_{TX}, \quad p_{0r} = p_{0RX} \end{aligned} \tag{7}$$

where

$$\begin{aligned} S_{TX} &= (E_{TX} + F_{TX})/2, \quad D_{TX} = (E_{TX} - F_{TX})/2 \\ S_{RX} &= (E_{RX} + F_{RX})/2, \quad D_{RX} = (E_{RX} - F_{RX})/2 \end{aligned} \tag{8}$$

The deviation of (7) is similar to the method in [6], and the diplexer polynomials for Type-II junction can refer to [6, Equation (11)].

The evaluation of the diplexer polynomials is carried out iteratively according to the following steps.

Step 1) Initialization: the RX and TX filters of the diplexer are synthesized independently using the proposed linear frequency transformation and well-established techniques available in the literature [13].

Step 2) follow the iteration steps available in the literature [6, Section IV.A, steps (2)–(5)], diplexer polynomials can be obtained. Note that the roots of the polynomial $(N(s) + D(s))/2 = S_{TX}(s)S_{RX}(s)$ (derived from (7)) should be computed for type-I junction in the step of new estimation of and S_{TX} and S_{RX}.

When diplexer polynomials are obtained, two methods can be used to synthesize coupling matrix of overall resonator diplexer. One method is to continue to follow the steps in [6, Section IV.B] using similarity-transformation techniques. We will present another method based on optimization techniques in next section.

3. COUPLING MATRIX SYNTHESIS OF DIPLEXER

3.1. Diplexer Responses Based on Coupling Matrix

Coupling path of the diplexer with two junctions (Figure 1) can be described using the normalized $(N + 3) \times (N + 3)$ coupling matrix suitable for three-port networks. This "$N + 3$" coupling matrix M is

defined by blocks including conventional $N \times N$ coupling matrix M_n [7]. N is the total number of resonators of the diplexer.

The coupling matrix may be used for the analysis and design of coupled resonator diplexers. The relation between S-parameters and "$N+3$" coupling matrix can be expressed [7]

$$S_{11} = 1+2j\left[A^{-1}\right]_{11}, \quad S_{21} = -2j\left[A^{-1}\right]_{21}, \quad S_{31} = -2j\left[A^{-1}\right]_{31} \tag{9}$$

Here, $A = [\Omega U_0 - jR_0 + M]$ and U_0 and R_0 are diagonal $(N+3)\times(N+3)$ matrices given in [7, Equation (3)].

Group delay characteristics and isolation (S_{23}) of diplexer network are not given in [7]. Assuming a lossless overall diplexer, the unitary condition of the scattering matrix imposes that

$$S_{12}\cdot S_{12}^* + S_{22}\cdot S_{22}^* + S_{32}\cdot S_{32}^* = 1, \quad S_{13}\cdot S_{13}^* + S_{23}\cdot S_{23}^* + S_{33}\cdot S_{33}^* = 1 \tag{10}$$

According to the symmetry of the scattering matrix, isolation (S_{23}) can be obtained from (10) as:

$$|S_{23}|^2 = 1 - |S_{21}|^2 - |S_{22}|^2, \quad \text{or} \quad |S_{23}|^2 = 1 - |S_{31}|^2 - |S_{33}|^2 \tag{11}$$

where $S_{22} = 1 + 2j[A^{-1}]_{22}$, $S_{33} = 1 + 2j[A^{-1}]_{33}$.

According the group delay in the Ω domain [14], we derive the actual value of the group delay in the physical frequency f domain as

$$\begin{aligned} \text{delay}(2,1) &= -\text{Im}\left(\frac{1}{S_{21}}\frac{\partial S_{21}}{\partial \Omega}\frac{\partial \Omega}{2\pi \partial f}\right), \\ \text{delay}(3,1) &= -\text{Im}\left(\frac{1}{S_{31}}\frac{\partial S_{31}}{\partial \Omega}\frac{\partial \Omega}{2\pi \partial f}\right) \end{aligned} \tag{12}$$

Group delay between the ports may now be expressed using (3) and (12) as follows

$$\text{delay}(m,1) = \text{Im}\left[\frac{\sum_{k=p+1}^{N+p}\left[A^{-1}\right]_{mk}\left[A^{-1}\right]_{k1}}{\left[A^{-1}\right]_{m1}}\right]\cdot\frac{f_0}{2\pi\cdot BW}\left(\frac{1}{f_0}+\frac{f_0}{f^2}\right), \quad m \in \{2,3\} \tag{13}$$

where p is the number of ports for the diplexer ($p = 3$). Note that, the "$N+3$" coupling matrix M can degenerate M_n for the Type-II diplexer, and then its S-parameters (only S_{11}, S_{21}, and S_{31}) can also be computed by the method in [8]. However, equation in [8] is invalid for the Type-I diplexer.

3.2. Coupling Matrix Synthesis Using Hybrid Optimization

Once the diplexer polynomials are determined based on the method in Section 2, the frequency response of the diplexer, as computed directly from in (2), is determined. The nonzero coupling matrix element M_{pq} are used as optimized variables and varying their values causes the response to change. The aim of the coupling matrix synthesis process is to select coupling matrix which produce a diplexer response by (9) coincide with the response obtained from (2).

To this purpose, the cost function is proposed as

$$E_{obj} = \sum_{k=1}^{N} |S_{11}(\Omega_{rk})|^2 + \sum_{i=1}^{T_1} |S_{21}(\Omega_{zi})|^2 + \sum_{j=1}^{T_2} |S_{31}(\Omega_{zj})|^2 + (|S_{11}(1)| - C_1)^2 + (|S_{11}(-1)| - C_{-1})^2 + (|S_{11}(\Omega_r)| - C_r)^2 + (|S_{11}(\Omega_t)| - C_t)^2 \,. \quad (14)$$

where Ω_{rk} is are the reflection zeros of the diplexer (the roots of $N(s)$ in Ω domain); Ω_{zi}, Ω_{zj} are the frequency locations of transmission zeros of S_{21}, S_{31}, respectively, T_1, T_2 are the numbers of the transmission zeros of S_{21}, S_{31} respectively C_1, C_{-1}, C_r and C_t are the absolute values of S_{11} at $\Omega = 1$, $\Omega = -1$, $\Omega = \Omega_r$ and $\Omega = \Omega_t$ respectively.

By minimizing the cost function in (14), the nonzero coupling matrix elements M_{pq} composing of the "$N + 3$" coupling matrix M can be obtained by a hybrid method. This hybrid method consists of a gradient-based SolvOpt algorithm [16] for a local optimizer and genetic algorithm [17, 18] for a global optimizer, respectively. A similar approach to the derivation of gradient of filter cost function in [19] has been adopted in this paper to derive the gradient of the cost function given in (14).

4. EXAMPLES OF DIPLEXERS SYNTHESIS AND DESIGN

For the verification of the diplexer synthesis method presented in this paper, two diplexers are synthesized, designed and measured.

4.1. Synthesis and Design of Diplexer with Type-I Junction (Diplexer 1)

A diplexer with Type-I junction is required to meet the following specifications:
***RX* Filter**: Number of poles (N_{RX}): 3; Band: 1.92–2.0033 GHz; Return loss (RL_{RX}): 20 dB; Transmission zeros (GHz): 1.8929.
***TX* Filter (all poles)**: Number of poles (N_{TX}): 3; Band: 2.1826–2.28 GHz; Return loss (RL_{TX}): 20 dB.

Table 1. The roots of the computed polynomials of diplexer 1.

k	Roots of $N(s)$	Roots of $D(s)$	Roots of $P_r(s)$	Roots of $P_t(s)$
1	$-0.9801i$	$-0.0686 - 1.0558i$	$-1.2137i$	$-0.0155 - 1.0695i$
2	$-0.8165i$	$-0.2641 - 0.8751i$	$-0.0577 + 1.1027i$	$-0.1473 - 0.8792i$
3	$-0.5904i$	$-0.1609 + 1.0919i$	$-0.1885 + 0.7468i$	$-0.1009 - 0.4979i$
4	$0.9632i$	$-0.3224 + 0.7253i$	$-0.0762 + 0.3850i$	-
5	$0.7250i$	$-0.1950 - 0.4560i$	-	-
6	$0.4868i$	$-0.1613 + 0.3576i$	-	-

$p_{0r} = 0.0683$, $p_{0t} = 0.0505$

Table 2. The synthesized coupling matrix of diplexer 1.

	P_1	P_2	P_3	1	2	3	4	5	6
P_1	0	0	0	0.5657	0	0	0.5159	0	0
P_2	0	0	0	0	0	0.5678	0	0	0
P_3	0	0	0	0	0	0	0	0	0.5135
1	0.5657	0	0	–0.7829	0.2777	0	0	0	0
2	0	0	0	0.2777	–0.7268	0.2832	0	0	0
3	0	0.5678	0	0	0.2832	–0.7249	0	0	0
4	0.5159	0	0	0	0	0	0.8008	0.1991	–0.1288
5	0	0	0	0	0	0	0.1919	0.9013	0.2021
6	0	0	0.5135	0	0	0	–0.1288	0.2021	0.7445

We obtain that the transmission zeros of RX filter locates at -1.95 in Ω' domain (corresponding -1.2138 in Ω domain) and $\Omega_r = -0.55$, $\Omega_t = 0.45$, $f_0 = 2.10\,\text{GHz}$; $BW = 0.36\,\text{GHz}$.

The roots of the computed diplexer polynomials are shown in Table 1.

After optimization using the method in Section 3.2, the obtained coupling matrix is shown in Table 2. The diplexer responses, obtained directly from the coupling matrix in Table 2, computed according to (9), (10) and (13), are shown in Figure 3.

The normalized coupling matrix must be de-normalized for using in the physical dimensioning of the diplexer. The de-normalized

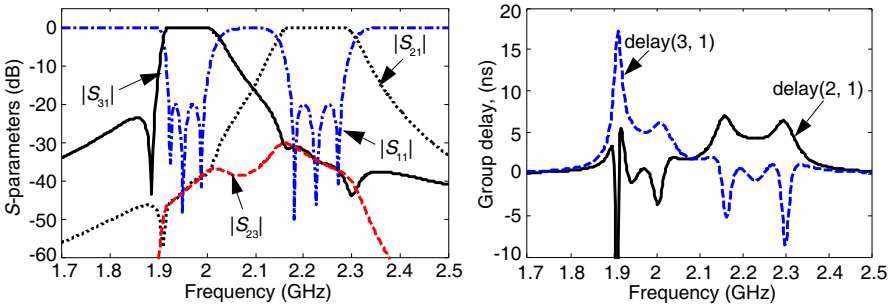

Figure 3. The synthesized responses of the diplexer 1, (a) S-parameters and (b) group delay.

coupling coefficients can be obtained via the following equation:

$$K_{ij} = FBW \cdot M(i,j), \quad i \neq j, \quad i, j = 1, 2, \ldots, N$$
$$f_{0i} = \frac{f_0\sqrt{K_{ii}^2 + 4} - f_0 K_{ii}}{2}, \quad i = 1, 2, \ldots, N \tag{15}$$
$$Q_{em} = \frac{1}{FBW \cdot M^2(p_k, m)}, \quad k = 1, 2, 3$$

where, FBW is the fractional bandwidth, $K_{ii} = M_{ii} \cdot FBW$, K_{ij} represents the coupling coefficient between resonators i and j. f_{0i} is the resonant frequency of the resonator i. Q_{em} is the external quality factor of the resonator m connected to the port p_k.

Figure 4(a) shows the coupling scheme of the diplexer 1. Using (15), the de-normalized coupling coefficients of the diplexer 1 are given as follows:

The coupling coefficients between resonators: $K_{1,2} = 0.0476$, $K_{2,3} = 0.0485$, $K_{4,5} = 0.0341$, $K_{5,6} = 0.0347$, $K_{4,6} = -0.0221$.

Resonance frequency for each resonator (GHz): $f_{0k} = \{2.2456, 2.2349, 2.2345, 1.9608, 1.9440, 1.9703\} k = 1, 2, \ldots, 6$.

External quality factors: $Q_{e1} = 18.229$, $Q_{e4} = 21.920$, $Q_{e3} = 18.092$ and $Q_{e6} = 22.121$.

After the coupling coefficients are determined, the next step requires the choice of proper resonator types to complete the diplexer design. In this design the half-wavelength open-loop resonators was chosen. The diplexer is designed to be fabricated on a Rogers RT/duroid 5880 substrate with a relative dielectric constant of 2.2, a thickness of 0.508 mm, and a loss tangent of 0.0009.

A full-wave simulator IE3D has been used to extract coupling coefficients K_{ij} and Q_e for initial sizes of the diplexer using the

method in [15]. In this diplexer design, 15 parameters, including 5 main couplings, 6 self-couplings, and 4 external Q values, need to be tuned to obtain the acceptable diplexer responses. To accelerate the diplexer design, the methods presented in [20, 21] can be applied to guide the tuning of each channel in the diplexer. After tuning, physical dimensions of the diplexer 1 are obtained as shown in Figure 4(b).

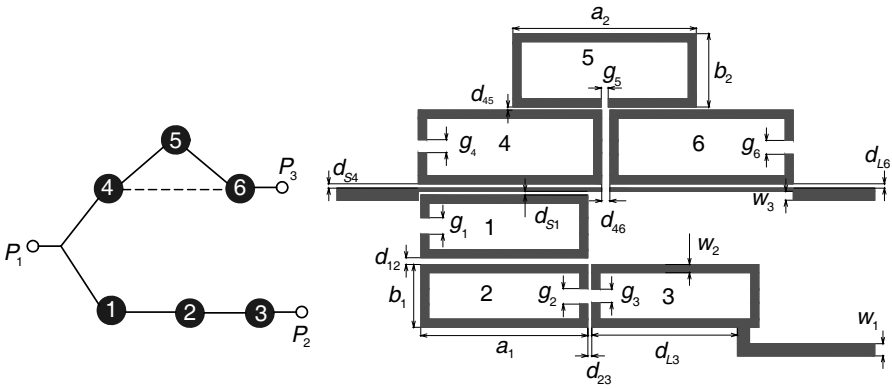

Figure 4. (a) Coupling scheme and (b) physical structure and dimensions of the diplexer 1. Associated dimensions (unit mm): $a_1 = 20.5$, $b_1 = 7.7$, $a_2 = 22.50$, $b_2 = 9.00$, $g_1 = 2.02$, $g_2 = 1.90$, $g_3 = 1.63$, $g_4 = 1.60$, $g_5 = 0.85$, $g_6 = 1.70$, $d_{S1} = 0.24$, $d_{S4} = 0.25$, $d_{L3} = 17.86$, $d_{L6} = 0.24$, $d_{12} = 0.83$, $d_{23} = 0.18$, $d_{45} = 0.41$, $d_{46} = 1.0$, $w_1 = 1.49$, $w_2 = 1.00$, $w_3 = 1.09$.

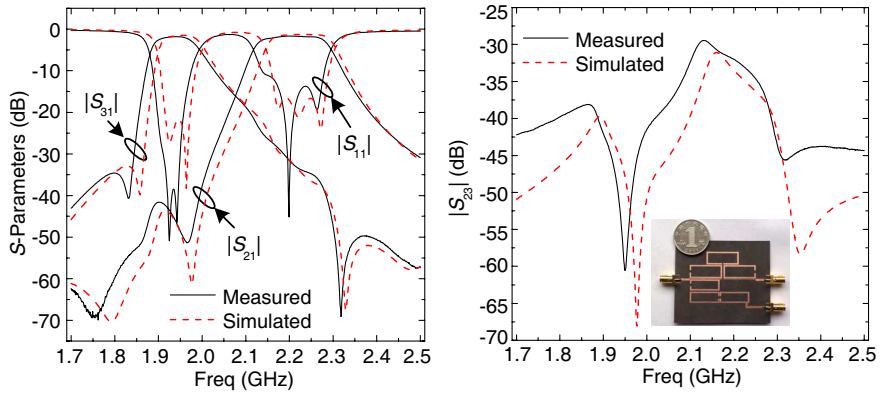

Figure 5. Measured and simulated S-parameters of the diplexer 1, (a) S_{21}, S_{11}, and S_{31}, and (b) isolation (S_{23}).

The diplexer has been simulated using a full-wave simulator IE3D. The loss factors (conductor loss and dielectric loss) are included in the simulated response. The measured S-parameters of the fabricated diplexer 1 are compared to the simulation one in Figure 5. Measured responses show a reasonably good agreement with the simulated responses. There is, however, a small frequency shift (about 17 MHz, 0.8% with respect to the center frequency), which can be attributed to the fabrication error or/and the change of permittivity.

4.2. Synthesis and Design of Diplexer with Type-II Junction (Diplexer 2)

A diplexer with Type-II junction is required to meet the following specifications:

***RX* Filter (all poles)**: Number of poles (N_{RX}): 3; Band: 2.4–2.4534 GHz; Return loss (RL_{RX}): 20 dB.

***TX* Filter**: Number of poles (N_{TX}): 5; Band: 2.5302–2.6 GHz; Return loss (RL_{TX}): 20 dB; Transmission zeros (GHz): 2.6328, 2.4986.

We obtain that the transmission zeros of TX filter locates at 1.9232, -1.9232 in Ω' domain (corresponding 1.3139, 0.0061 in Ω domain) and $\Omega_r = -0.45$, $\Omega_t = 0.32$, $f_0 = 2.498$ GHz; $BW = 0.20$ GHz.

After obtaining polynomials and optimization using the method in Sections 2 and 3.2, the obtained coupling matrix is shown in Table 3. The diplexer responses, obtained directly from the coupling matrix in Table 3, computed according to (9), (10) and (13), are shown in Figure 6.

The de-normalized coupling coefficients are determined using (15), and then the square half-wavelength open-loop resonators are chosen to

Table 3. The synthesized coupling matrix of diplexer 2.

	1	2	3	4	5	6	7	8	9
1	0	0.7967	0	0	0	0	0.7754	0	0
2	0.7967	−0.6320	0.2632	0	0	0	0	0	0
3	0	0.2632	−0.6548	0.2077	0	-0.0391	0	0	0
4	0	0	0.2077	−0.6558	0.2394	0	0	0	0
5	0	0	0	0.2394	−0.6583	0.2912	0	0	0
6	0	0	−0.0391	0	0.2912	−0.6566	0	0	0
7	0.7754	0	0	0	0	0	0.6928	0.2594	0
8	0	0	0	0	0	0	0.2594	0.7183	0.2854
9	0	0	0	0	0	0	0	0.2854	0.7194

$M(p_1, 1) = 1.4777$; $M(p_2, 6) = 0.5951$; $M(p_3, 9) = 0.5739$

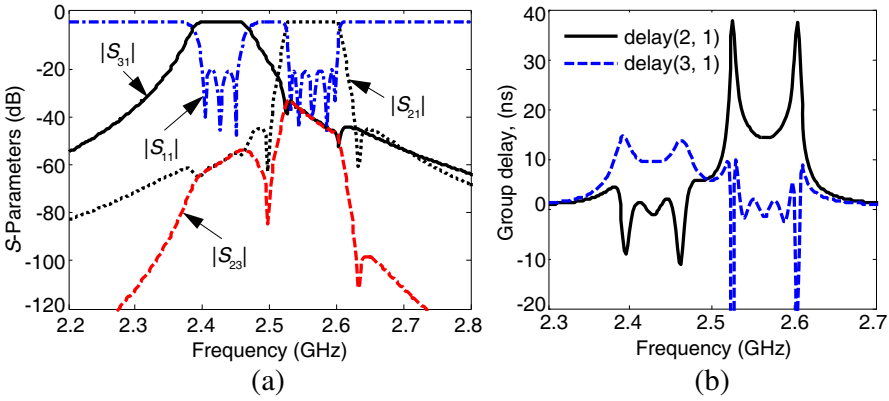

Figure 6. The synthesized responses of the diplexer 2, (a) S-parameters and (b) group delay.

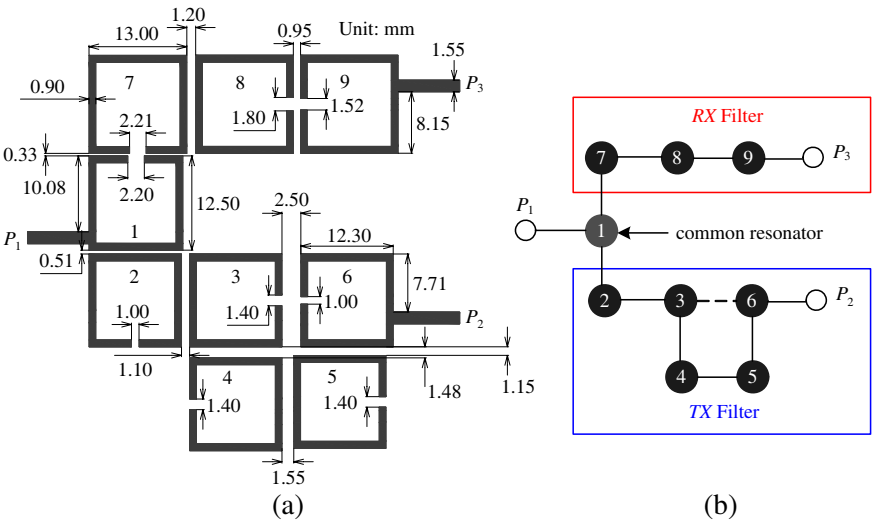

Figure 7. (a) The physical structure and dimensions and (b) coupling scheme of the diplexer 2.

complete the design. The diplexer is designed using the same substrate as diplexer 1. In this diplexer design, 21 parameters, including 9 main couplings, 9 self-couplings, and 3 external Q values, need to be tuned to obtain acceptable diplexer responses. The methods presented in [20, 21] can be applied to guide the tuning of each channel in the diplexer. After tuning, physical dimensions of the diplexer 2 are obtained as shown in Figure 7(a). Figure 7(b) shows the coupling scheme of the diplexer 2.

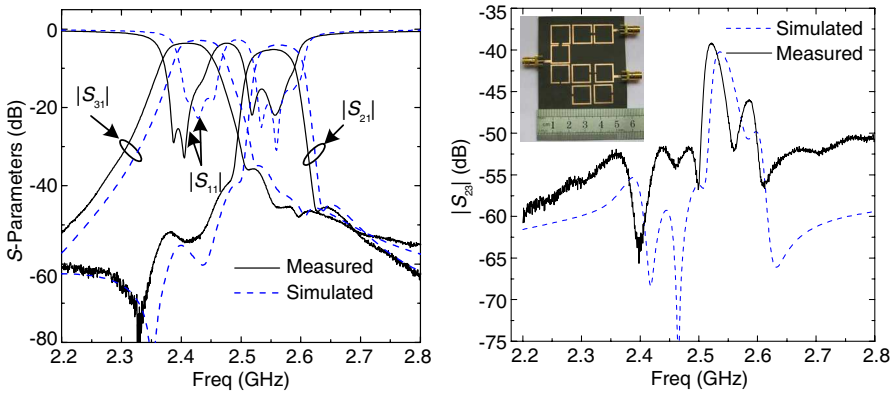

Figure 8. Measured and simulated S-parameters of the diplexer 2, (a) S_{21}, S_{11}, and S_{31}, (b) isolation (S_{23}). Photograph of the fabricated diplexer is inserted.

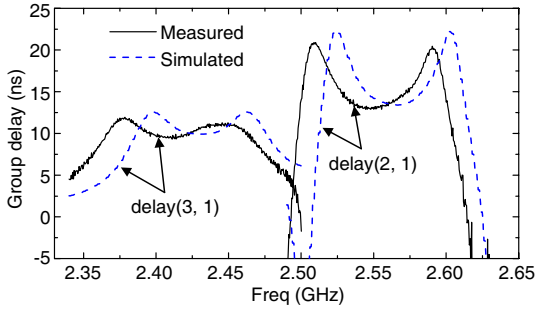

Figure 9. Measured and simulated group delay of the diplexer 2.

Figures 8 and 9 show the measured and simulated S-parameters and group delay, respectively. Measured responses show a reasonably good agreement with the simulated responses. There is, however, a small frequency shift (about 16 MHz, 0.64% with respect to the center frequency), which can be attributed to the fabrication error or/and the change of permittivity.

5. CONCLUSION

A novel approach to the synthesis of microwave resonator diplexers with two-type junctions has been presented. A linear frequency transformation is proposed for the evaluation of the characteristic polynomials of the diplexer, and then coupling matrix of overall

diplexer can be obtained using the proposed hybrid optimization methods combining a gradient-based SolvOpt and a genetic algorithm. The evaluation of group delay in the physical frequency f domain and isolation (S_{23}) based on coupling matrix are derived. To illustrate the validation of the method, two examples, including 6-poles diplexer with Type-I junction and 9-poles diplexer with Type-II junction, have been synthesized, designed, simulated, and measured.

ACKNOWLEDGMENT

This work was supported by the Fundamental Research Funds for the Central Universities of China (ZYGX 2009J041 and ZYGX2010J046).

REFERENCES

1. Yang, T., P. L. Chi, and T. Itoh, "High isolation and compact diplexer using the hybrid resonators," *IEEE Microw. Wireless Compon. Lett.*, Vol. 20, No. 10, 551–553, Oct. 2010.
2. Shi, J., J.-X. Chen, and Z.-H. Bao, "Diplexers based on microstrip line resonators with loaded elements," *Progress In Electromagnetics Research*, Vol. 115, 423–439, 2011.
3. Yang, R.-Y., C.-M. Hsiung, C.-Y. Hung, and C.-C. Lin, "Design of a high band isolation diplexer for GPS and WLAN system using modified stepped-impedance resonators," *Progress In Electromagnetics Research*, Vol. 107, 101–114, 2010.
4. Huang, C.-Y., M.-H. Weng, C.-S. Ye, and Y.-X. Xu, "A high band isolation and wide stopband diplexer using dual-mode stepped-impedance resonators," *Progress In Electromagnetics Research*, Vol. 100, 299–308, 2010.
5. Morini, A. and T. Rozzi, "Constraints to the optimum performance and bandwidth limitations of diplexers employing symmetric three-port junctions," *IEEE Trans. Microw. Theory Tech.*, Vol. 40, No. 2, 242–248, Feb. 1996.
6. Macchiarella, G. and S. Tamiazzo, "Novel approach to the synthesis of microwave diplexers," *IEEE Trans. Microw. Theory Tech.*, Vol. 54, No. 12, 4281–4290, Dec. 2006.
7. Garcia-Lamperez, A., M. Salazar-Palma, and T. K. Sarkar, "Analytical synthesis of microwave multiport networks," *IEEE MTT-S Int. Microwave Symp. Digest*, 455–458, USA, Jun. 2004.
8. Skaik, T. F., M. J. Lancaster, and F. Huang, "Synthesis of multiple output coupled resonator circuits using coupling matrix optimisation," *IET Microwaves, Antennas & Propagation*, Vol. 5, No. 9, 1081–1088, 2011.

9. Skaik, T. F. and M. J. Lancaster, "Coupled resonator diplexer without external junctions," *Journal of Electromagnetic Analysis and Applications*, Vol. 3, No. 6, 238–241, 2011.
10. Chen, C.-F., T.-Y. Huang, C.-P. Chou, and R.-B. Wu, "Microstrip diplexer design with common resonator section for compact size but high isolation," *IEEE Trans. Microw. Theory Tech.*, Vol. 54, No. 5, 1945–1952, May 2006.
11. Chuang, M. L. and M.-T. Wu, "Microstrip diplexer design using common T-shaped resonator," *IEEE Microw. Wireless Compon. Lett.*, Vol. 21, No. 11, 583–585, Nov. 2011.
12. Yang, T. P., L. Chi, and T. Itoh, "Compact quarter-wave resonator and its applications to miniaturized diplexer and triplexer," *IEEE Trans. Microw. Theory Tech.*, Vol. 59, No. 2, 260–269, Feb. 2011.
13. Cameron, R. J., "Advanced coupling matrix techniques for microwave," *IEEE Trans. Microw. Theory Tech.*, Vol. 51, No. 1, 1–10, Jan. 2003.
14. Amari, S., "Synthesis of cross-coupled resonator filters using an analytical gradient-based optimization technique," *IEEE Trans. Microw. Theory Tech.*, Vol. 48, No. 9, 559–1564, Sep. 2000.
15. Hong, J.-S. and M. J. Lancaster, *Microstrip Filter for RF/Microwave Applications*, 235–271, Wiley, New York, 2001.
16. SolvOpt manual and SolvOpt Toolbox for matlab, Available: http://www.kfunigraz.ac.at/imawww/kuntsevich/solvopt/index.html.
17. GA Toolbox, http://www.shef.ac.uk/acse/research/ecrg/getgat.html.
18. Uhm, M., S. Nam, and J. Kim, "Synthesis of resonator filters with arbitrary topology using hybrid method," *IEEE Trans. Microw. Theory Tech.*, Vol. 55, No. 10, 2157–2167, Oct. 2007.
19. Amari, S., R. Rosenberg, and J. Bornemann, "Adaptive synthesis and design of resonator filters with source/load-multiresonator coupling," *IEEE Trans. Microw. Theory Tech.*, Vol. 50, No. 8, 1969–1978, Aug. 2002.
20. Wang, R. and J. Xu, "Extracting coupling matrix and unloaded Q from scattering parameters of lossy filters," *Progress In Electromagnetics Research*, Vol. 115, 303–315, 2011.
21. Wang, R., J. Xu, C. L. Wei, M.-Y. Wang, and X.-C. Zhang, "Improved extraction of coupling matrix and unloaded Q from S-parameters of lossy resonator filters," *Progress In Electromagnetics Research*, Vol. 120, 67–81, 2011.